HHS Public Access

Author manuscript

Cell Rep. Author manuscript; available in PMC 2022 November 17.

Published in final edited form as:

Cell Rep. 2022 October 25; 41(4): 111547. doi:10.1016/j.celrep.2022.111547.

Circadian transcriptional pathway atlas highlights a proteasome switch in intermittent fasting

Fang Wei[1,5], **Lijun Gong**[1,5], **Siyu Lu**[1], **Yiming Zhou**[1], **Li Liu**[1], **Zhigui Duan**[1], **Rong Xiang**[3], **Frank J. Gonzalez**[4], **Guolin Li**[1,2,6,*]

[1]Center for Biomedical Aging, National & Local Joint Engineering Laboratory of Animal Peptide Drug Development, College of Life Sciences, Hunan Normal University, Changsha, Hunan 410081, China

[2]Key Laboratory of Hunan Province for Model Animal and Stem Cell Biology, School of Medicine, Hunan Normal University, Changsha, Hunan 410081, China

[3]Department of Cell Biology, School of Life Sciences, Central South University, Changsha, Hunan 41001, China

[4]Laboratory of Metabolism, Center for Cancer Research, National Cancer Institute, National Institutes of Health, Bethesda, MD 20892, USA

[5]These authors contributed equally

[6]Lead contact

SUMMARY

While intermittent fasting is a safe strategy to benefit health, it remains unclear whether a "timer" exists *in vivo* to record fasting duration and trigger a transcriptional switch. Here, we map a circadian transcriptional pathway atlas from 600 samples across four metabolic tissues of mice under five feeding regimens. Results show that 95.6% of detected canonical pathways are rhythmic in a tissue-specific and feeding-regimen-specific manner, while only less than 25% of them induce changes in transcriptional function. Fasting for 16 h initiates a circadian resonance of 43 pathways in the liver, and the resonance punctually switches following refeeding. The hepatic proteasome coordinates the resonance, and most genes encoding proteasome subunits display a 16-h fasting-dependent transcriptional switch. These findings indicate that the hepatic proteasome may serve as a fasting timer and a coordinator of pathway transcriptional resonance, which provide a target for revealing the underlying mechanism of intermittent fasting.

Graphical Abstract

*Correspondence: hnsdlgl@hunnu.edu.cn.

AUTHOR CONTRIBUTIONS

G.L. designed the experiments. G.L., F.W., L.G., S.L., Y.Z., L.L., and Z.D. conceived experiments. G.L. performed the bioinformatics analysis. G.L., F.W., and R.X. contributed to the interpretation of results. G.L., F.W., and F.J.G. wrote the manuscript.

DECLARATION OF INTERESTS

The authors declare no competing interests.

SUPPLEMENTAL INFORMATION

Supplemental information can be found online at https://doi.org/10.1016/j.celrep.2022.111547.

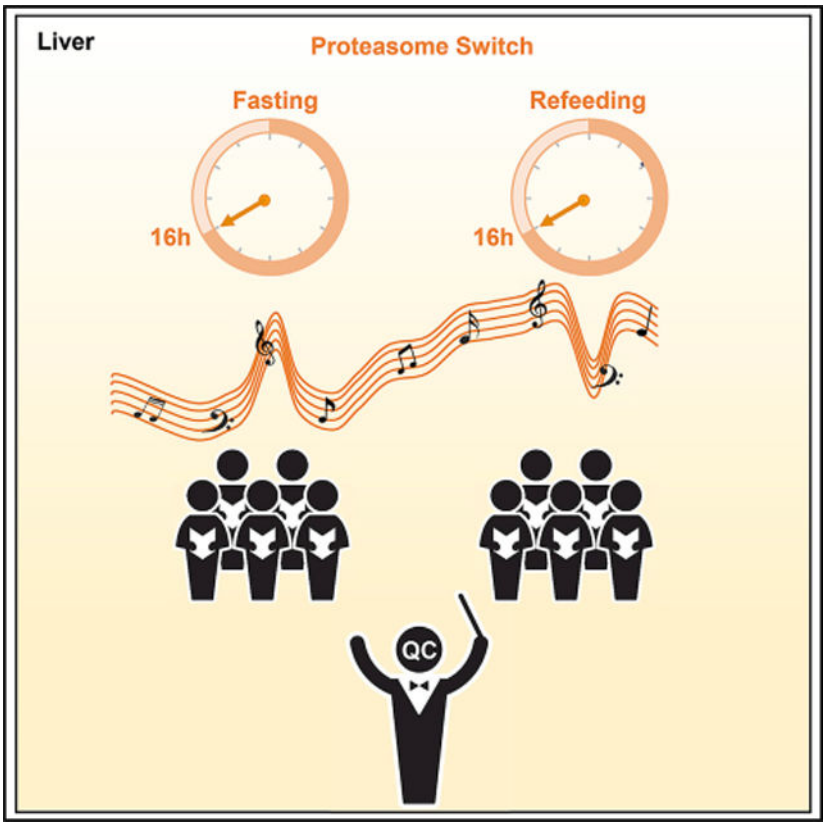

In brief

While intermittent fasting benefits health, the optimal duration of each fasting remains an open question. Wei et al. map an atlas of canonical pathways in intermittent fasting, find that fasting for 16 h initiates circadian resonance of pathways in the liver, and identify the proteasome as a liver-specific fasting “timer”.

INTRODUCTION

Intermittent fasting has become a safe strategy to benefit health (de Cabo and Mattson, 2019; Stekovic et al., 2019). Growing evidence consistently shows that intermittent fasting can efficiently prevent a wide range of diseases, including diabetes, obesity, cancers, and neurodegenerative disorders (Di Francesco et al., 2018; Li et al., 2017; Nencioni et al., 2018). It even functions to increase lifespan or retard the aging process in different animal models (Anton et al., 2018; Catterson et al., 2018; Honjoh et al., 2009; Longo et al., 2021; Ulgherait et al., 2021; Xie et al., 2017). However, there are currently many intermittent fasting regimens (Anton et al., 2018; de Cabo and Mattson, 2019; Longo et al., 2021), while the strong evidence of exclusivity for the predominance of each regimen is limited. The temporal functional signatures of fasting remain to be elucidated.

It is assumed that flipping the metabolic switch from glucose to fatty-acid-derived ketones is a key mechanism responsible for the intermittent-fasting-induced health benefits (Anton et al., 2018; de Cabo and Mattson, 2019; Mattson et al., 2018), and plasma ketone levels

can serve as a biomarker of the metabolic switch (Anton et al., 2018). While there is a wide consensus that prolonged fasting can trigger the metabolic switch, and multifaceted evidence supports a crucial role of the metabolic switch in optimizing metabolism and improving metabolic diseases, the metabolic switch that occurs between 12 and 36 h after food deprivation varies greatly between individuals (Anton et al., 2018). In this context, it is difficult for the metabolic switch to accurately indicate functional switches at a given time point, and two open questions that arise are whether a "timer" exists *in vivo* to record the fasting duration, and whether and when does fasting spark transcriptional switches?

Theoretically, these temporal signatures should be associated with circadian clocks. Intriguingly, multiple lines of evidence have supported the interaction between circadian rhythms and intermittent fasting. Circadian clocks optimize the benefits of intermittent fasting through temporally orchestrating signaling pathways, metabolic activity, and other cellular functions (Manoogian and Panda, 2017; Mohawk et al., 2012). In turn, feeding behavior modifications in energy components and time can markedly alter rhythmic transcription (Greenwell et al., 2019; Kohsaka et al., 2007; Villanueva et al., 2019; Vollmers et al., 2009). Feeding-regulated hormones and metabolic oscillators can reset circadian rhythms *in vivo* (Bass, 2012; Crosby et al., 2019; Peek et al., 2013). Time-restricted feeding prevents metabolic diseases even in mice lacking a circadian clock (Chaix et al., 2019), while mistimed eating has deleterious effects on metabolic health (Challet, 2019). However, data from current transcriptomics studies have not revealed a transcriptional switch or fasting timer. In this case, we suspect that the temporal signatures may be tissue specific and present at the pathway level rather than the gene level.

Therefore, in the current study, with the use of gene set variation analysis (GSVA) (Hanzelmann et al., 2013) and canonical pathways gene sets (Mootha et al., 2003; Subramanian et al., 2005), we mapped a circadian transcriptional pathway atlas based on 600 samples across four metabolic tissues sampled every 4 h from mice placed on *ad libitum* (AL), acute fasting (AF), refeeding after acute fasting (AR), every-other-day fasting (EODF), and every-other-day refeeding (EODR) regimens. The evidence suggests that intermittent fasting significantly triggers liver-specific transcriptional switches of 43 canonical pathways after 16-h fasting or refeeding, and the liver proteasome may serve as a potential fasting timer and coordinator of pathway switches.

RESULTS

Canonical pathway profiling of mouse tissues reveals tissue-specific oscillating signatures in intermittent fasting

To determine the adaptive metabolic changes induced by intermittent fasting, the effect of EODF on body weight was first analyzed. Compared with the AL group, EODF did reduce the body mass gain (Figure S1). To obtain a comprehensive metabolic perspective of the temporal signature of intermittent fasting, we measured the transcriptome of four metabolic tissues (liver, skeletal muscle [biceps femoris], interscapular brown adipose tissue [BAT], and inguinal white adipose tissue [WAT]) isolated every 4 h from mice placed on AL, AF, AR, EODF, or EODR regimens (Figure 1A). RNA sequencing identified the expression of 17,848 genes at least in one group (Table S1), and the transcriptome measurements were

highly accurate and reproducible, with Spearman correlation coefficients more than 0.95 in biological replicates (Figures S2A and S2B) and more than 0.80 in samples across groups (Figures S2A and S2C).

Three-dimensional (3D) principal-component analysis (PCA) (Venables and Ripley, 2002) of transcriptomic data did not classify each group according to different feeding regimens (Figure S2D), indicating that it might be difficult to find the temporal signature of intermittent fasting at the gene level. Therefore, we further calculated pathway GSVA scores (Hanzelmann et al., 2013) for these genes based on 2,922 gene sets of canonical pathways that were downloaded from the MSigDB (c2.cp.v7.4) (Mootha et al., 2003; Subramanian et al., 2005). We identified 2,175 pathways at least in one group (Table S2), accounting for 74.4% of total pathways. Most (2,007 in 2,175) were commonly enriched in all four tissues (Table S2). Further 3D-PCA analysis with the GSVA scores improved the classification of samples across feeding regimens, but some samples still overlapped (Figure S2E). Given that more than half of the nuclear receptors and the majority of protein-coding genes exhibit rhythmic expression (Mure et al., 2018; Yang et al., 2006; Zhang et al., 2014), we suspected that pathways composed of multiple genes might also display rhythmic features and the effects of feeding regimens on pathways might be masked by the features.

As expected, we observed an obvious tissue-specific and feeding-regimen-specific circadian oscillation in canonical pathways (Figure 1B). In skeletal muscle of AL mice, the majority of pathways were upregulated in the dark cycle but downregulated in the light cycle (Figures 1B and 1C), which is synchronized with the characteristics that this nocturnal species is most active at night. The ratio of the dark cycle to the light cycle of upregulated pathways illustrated that skeletal muscle and WAT were more sensitive to AF than the other two tissues (Figure 1C). Further comparative analysis of circadian oscillating pathways revealed the effects of different feeding regimens on these pathways were tissue specific, and the total number of oscillating pathways varied among tissues (Figure 2). In AL mice, the percentage of oscillating pathways in muscle was just 8%, while that in other tissues was more than 25% (Figure 2). These data are consistent with previous evidence that 15% of hepatic transcripts and 4% of muscle transcripts were cyclic (Kinouchi et al., 2018). Compared with AL mice, all other feeding regimens tended to decrease the percentage of oscillating pathways in the liver and WAT, but, in muscle and BAT, the decrease only occurred in a specific feeding regimen (Figure 2). The correlations, amplitude, and phase distribution of oscillating pathways among different feeding regimens also showed tissue-specific signatures (Figure 2). It was reported that fasting can cease the oscillation of more than 60% of rhythmic transcripts in the liver and muscle (Kinouchi et al., 2018). Accordingly, we noticed that the oscillating pathway correlations of AL with AF in the liver and muscle were very low (Figure 2). If we considered the phase, there were few overlapping pathways between AL and AF (Figure 2; Table S3). Due to the low overlap of cyclic pathways among feeding regimens and tissues, a total of 2,079 rhythmic pathways were detected at least in a specific feeding regimen of one tissue (Table S3), which accounts for 95.6% of the 2,175 identified pathways (Table S2). Considering the high rhythmicity of genomic transcription (Mure et al., 2018) and the potential influence of feeding behavior on rhythmic transcription (Vollmers et al., 2009), the high oscillation of these pathways is logical. Notably, the phases in AF mice seemed to be chronological among different tissues: WAT peaked at 8–10 h after

fasting, then BAT at 12 h, liver at 20 h, and muscle at 22 h (Figure 2), suggesting that the length of fasting time to initiate a response is also tissue specific. All these data indicate that canonical pathways are highly rhythmic, and intermittent fasting can spin oscillating signatures of these pathways in a tissue-specific manner.

Canonical pathway profiling all day suggests an adaptation to "acute fasting-refeeding" in intermittent fasting

Owing to the high rhythmicity of genomic transcription and canonical pathways, to precisely evaluate the effects of different feeding regimens on these pathways, the overlapping effects of circadian oscillation on the data should first be eliminated. Thus, the mean expression values (*EDi*) of each gene for the whole day were calculated from the expression values (*Eij*) of six time points in a 24-h day within each feeding regimen and tissue (Figure 3A). The means were then used for GSVA, 3D-PCA, and other analyses.

Based on these means, we did observe that different feeding regimens caused mild and clear alterations in the transcripts (Figure 3B) and canonical pathways (Figure 3C), respectively, as indicated by the generalized 3D-PCA distances. Surprisingly, different tissues appeared to have coordinated responses to intermittent fasting, as the Spearman correlation coefficients of canonical pathways exhibited similar patterns of change across tissues (Figure 3D); that is, the coefficients within each feeding regimen were apparently positive, while those between AF and EODR or between AR and EODF were obviously negative (Figure 3D). These data challenged our conventional view that AF and AR or EODF and EODR are two pairs of inverse effects. Especially, the coefficients between AF and AR in muscle, and those between EODF and EODR in muscle, WAT, and BAT were positive (Figure 3D). These results can be compared with the classic concept of ischemic-reperfusion injury. Although the restoration of blood flow (reperfusion) is a routine means of handling tissue ischemia, some functional and structural changes become apparent during reperfusion after a period of ischemia (Soares et al., 2019). Therefore, these data indicate that acute fasting-refeeding might be a pair of linked nutritional challenges, and that intermittent fasting, by adapting to the challenges, may yield beneficial effects on an organism.

The functional rhythmic pathways exhibit a manifest switch after 16 h fasting or refeeding in the liver

Since the pathway GSVA scores refer to genes in pathways that are concordantly over-expressed or under-expressed and are approximately normal (Hanzelmann et al., 2013), we performed differential expression analysis on the whole-day GSVA scores using limma (Smyth, 2004). With the cutoff of $\log_2(\text{fold change}) > \log_2(1.5)$ and adjustedp < 0.05, we detected 1,343 differentially expressed pathways (DEPs) at least in one compared pair of a tissue (Table S4). The overlapping analysis within each tissue illustrated that only 16.6%–24.9% of rhythmic pathways overlapped with DEPs (Figures 4A–4D), indicating that most rhythmic pathways did not cause changes in transcriptional function throughout the whole day. These pathways showing both oscillation and differential expression will be referred to as functional rhythmic pathways (FRPs) in the following descriptions.

To explore the detailed oscillating characteristics of these FRPs, we first drew their heatmaps with GSVA scores calculated from the original expression data (Table S2). Intriguingly, the heatmap in the liver demonstrated an obvious expression switch at the 16th hour of fasting or refeeding (Figure 4E, black arrow), while that did not occur in other tissues (Figures 4F–4H) or the liver of AL mice (Figure 4E, black arrow). These results indicate that there is a liver-specific timer *in vivo* to record the duration of fasting and refeeding.

Therefore, we further analyzed the feeding-specificity and phase distribution of FRPs within each tissue. Results demonstrated that the major FRPs were clustered into AL and acute fasting-refeeding (Figures 5 [top bar charts] and S3A). Since an oscillating pathway that only occurs in AL mice actually represents a pathway that loses rhythmicity during AF and cannot restore rhythmicity in other feeding regimens, it also reflects the effect of AF. In this context, these data suggest that most of the overlapping pathways might directly stem from the AF-induced circadian fluctuations or indirectly derive from the adaptation to the AF-induced circadian fluctuations.

At each time point, the fraction of feeding-regimen-specific DEPs in FRPs fluctuated (Figure 5 [side bar charts]). Compared with the top bar charts, the proportion of EODF and EODR increased in the side bar charts, while that of AF decreased (Figure 5), indicating intermittent-fasting-induced changes in transcriptional function (as indicated by DEPs) originated more from the adaptation to AF-induced circadian fluctuation than from itself. Curiously, the peak at the 16th hour observed above (Figure 4E) did not appear, while the peak of FRPs varied across feeding regimens (Figures 5 [last column] and S3B). However, consistent with the above results (Figure 3D), we noticed several pairs of typical inverse effects between AR and EODF in DEPs of different tissues at the same oscillating time point (Figure 5 [green arrow]), and most of these pairs occurred in the rhythmic pathways of AF mice. The phase distribution of FRPs in AF mice highlighted the temporal effects of fasting in the liver, as only the liver sharply peaked at a single time point, the 20th hour of fasting (Figures S3C–S3F). Therefore, the pathways displaying inverse effects between AR and EODF at the 20th hour of fasting in the liver were chosen for further analysis. Intriguingly, of the 45 pathways upregulated in AR mice and 57 pathways downregulated in EODF mice (Figure 5 (green arrow)), 43 pathways were shared by both, which accounts for 18.8% of the total 229 FRPs in the liver (Figure 4A). The oscillating curves of the 43 pathways displayed a typic circadian resonance (Figure 6A). Although the fitted curve in AF mice peaked at the 20th hour of fasting, almost all pathways were clearly switched at the 16th hour of fasting (Figure 6A), which might explain the discrepancy between the peak of FRPs (Figure 5) and the switching time of the heatmap (Figure 4E). Consistent with the above data (Figure 4E), these 43 pathways only oscillated in fasting or refeeding mice, but not in AL mice (Figure 6A). Moreover, across feeding regimens, the switching time was fixed at the 16th hour of fasting or refeeding (Figure 6A). These data therefore confirm our assumption that intermittent fasting may trigger transcriptional switches at the pathway level.

The circadian resonance of 43 pathways in the liver highlights a proteasome switch in intermittent fasting

While the circadian resonance of 43 pathways is interesting, the question that arises is why does this happen? To answer this question, we first classified these pathways according to the Reactome Pathway Database (Jassal et al., 2020), as most of the 43 pathways were Reactome pathways. The results revealed that, although 42% belonged to signal transduction, their functions were distributed over several categories (Figure 6B). Obviously, they cannot be classified into one functional class.

Then, the genes that constituted these pathways were extracted for overlap analysis. Of the total of 837 genes, 14 were shared by all 43 pathways (Figure 6C). Surprisingly, they all are genes encoding proteasome subunits (Figure 6C), implying that the proteasome may coordinate the circadian resonance of these pathways. If it is the case, the transcription of the genes encoding proteasome subunits would be expected to be switched at the time after fasting or refeeding for 16 h. To verify this assumption, the transcription data of all genes encoding proteasome subunits were extracted for oscillation analysis. As expected, the expression of these genes in the liver did switch at the time point in fasting or refeeding (Figure 7A), which did not occur in other tissues (Figures 7B–7D). Consistent with the concept that the amount of proteasomes in Mammalia is regulated at the transcriptional level (Meiners et al., 2003), the expression of three proteins encoded by *Psma4*, *Psmb3*, and *Psmb6* in the liver that were randomly selected out from 14 shared genes in Figure 6C were also oscillated in a similar manner with the transcription of proteasome subunits (Figures 7E and S4A–S4E). These data suggest that the liver proteasome may be a fasting timer that coordinates the resonance of the 43 pathways. Since the proteasome plays a prominent role in the control of multiple basic cellular activities (Tanaka, 2009), this may explain why the 43 pathways belong to several categories.

One question that remains is whether the time point of a transcriptional switch is unique to fasting (refeeding) duration or the combined effect of dark/light switch and fasting (refeeding) duration. Fortunately, the data from a paper published in *Cell Reports* may be helpful to answer this question. In contrast to our fasting protocol that used a fixed start time point, that study fasted six groups of mice at six start time points with a 4-h interval between each (Kinouchi et al., 2018). Following this protocol, mice that were killed every 4 h over a day were all fasted for 24 h. Therefore, if fasting duration solely determines the transcriptional switch, the switching phenotype will be lost in these mice. As expected, the genes encoding proteasome subunits in these mice did not show obvious transcriptional switch at zeitgeber time 4 h or other times in the liver (Figure S5A), although some genes displayed transcriptional changes after fasting. Therefore, it might be logical to consider the transcriptional switch in these genes as a fasting-specific effect. Nevertheless, the fasting-induced transcriptional changes of some genes in muscle exhibited a seeming oscillatory effect (Figure S5B), suggesting a tissue-specific role for fasting. Together, these data indicate that it is the 16-h fasting that initiates the transcriptional switch of genes encoding proteasome subunits in the liver.

There is a wide consensus that prolonged fasting can promote the production of ketone bodies (Balasse and Fery, 1989). Recent evidence suggests that ketones serve as an

important signal in hepatic response to fasting (Geisler et al., 2019) and a key mechanism responsible for the intermittent-fasting-induced health benefits (Anton et al., 2018; de Cabo and Mattson, 2019; Mattson et al., 2018). To explore the potential role of ketones in intermittent-fasting-induced transcriptional switches, the oscillations in serum ketone bodies across the different groups were analyzed. The results showed that fasting increased serum acetoacetate and β-hydroxybutyrate levels (Figures S6A and S6B; Table S5), but they did not display obvious oscillations during fasting (Figures S6A and S6B; Table S5). These data suggest that ketone signaling should not orchestrate the transcriptional switches, and, therefore, our current evidence indicates that it is proteasome rather than ketone signaling that serves as a fasting timer.

DISCUSSION

In this study, we mapped the circadian transcriptional pathway atlas in four metabolic tissues of mice under five feeding regimens (AL and four components of intermittent fasting), which serves as an important resource for revealing the regulatory mechanism of intermittent fasting. Current evidence highlighting the importance of circadian rhythm in the beneficial effects of intermittent fasting (specifically time-restricted feeding) on health has been repeatedly reported (Chaix et al., 2019; Crosby et al., 2019; Greenwell et al., 2019; Manoogian and Panda, 2017; Ulgherait et al., 2021; Villanueva et al., 2019; Vollmers et al., 2009). Although the circadian transcriptome atlases in mice and primates have been mapped (Mure et al., 2018; Zhang et al., 2014) and rhythmic feeding has been shown to trigger the oscillations in most peripheral tissues (Damiola et al., 2000; Stokkan et al., 2001), the pathway atlas across major metabolic tissues of mice under intermittent fasting is still lacking. Here, we created high-resolution multi-organ transcriptional over-expression or under-expression of canonical pathways (Mootha et al., 2003; Subramanian et al., 2005) based on the GSVA analysis (Hanzelmann et al., 2013), and then characterized these pathways by oscillating signature and differential expression throughout the whole day. The data revealed that the transcriptional pathways were highly rhythmic, and the oscillating signature of these pathways was tissue specific and varied dramatically across feeding regimens. Although the oscillating pathways in muscle and WAT were more sensitive to AF than the other two tissues, BAT accounted for the most DEPs. These data imply that the changes in circadian oscillation of pathways cannot directly deduce the corresponding changes in transcriptional function. In fact, we found that only less than 25% of the oscillatory pathways lead to changes in transcriptional function all day.

A striking finding from this study is that fasting for 16 h can awake a liver-specific cellular quality controller (the proteasome). Although intermittent fasting has been proved to benefit health from many aspects, fasting programs vary across laboratories (Chaix et al., 2019; Li et al., 2017; Mihaylova et al., 2018; Ulgherait et al., 2021) and even within each laboratory (Chaix et al., 2019; Hatori et al., 2012; Villanueva et al., 2019). The main reason is that the exact time point *in vivo* at which organisms exhibit an apparent response to fasting has not been found. Here, we revealed that fasting for 16 h triggered an evident switching effect of many canonical pathways, and that, once this effect is initiated, the trough and peak would punctually occur in the following refeeding and fasting. Intriguingly, all the shared genes of these pathways were genes encoding proteasome subunits, indicating

the proteasome coordinated the pathway switches. Moreover, almost all genes encoding proteasome subunits in the liver demonstrated a fasting-dependent transcriptional switch similar to these pathways, indicating that the proteasome might be a liver-specific fasting timer. Although these data cannot directly imply that the fasting-induced switching effects in canonical pathways stem from those in the proteasome, the high synchronization of the transcriptional switch of these pathways and genes implies they are closely associated with each other. Since the proteasome is a critical component of cellular quality control systems (Pohl and Dikic, 2019; Tanaka, 2009), and previous evidence suggests a crucial role for fasting in increasing the activity of the proteasome and promoting selective degradation of specific proteins (VerPlank et al., 2019), the regulation of proteasome-coordinated pathways by fasting and refeeding implies that intermittent fasting may benefit health from the improved function of the cellular quality control systems. Although an open question remains for the mechanism of the pulse-like upregulation and downregulation of genes and pathways at a single time point in response to fasting and refeeding, respectively, this finding highlights the essential position of 16-h fasting in the beneficial role of intermittent fasting. Consistent with this notion, recent evidence indicates that fasting for more than 16 h is necessary for extending the lifespan of *Drosophila* (Ulgherait et al., 2021), and the underlying mechanism for the lifespan extension is circadian-regulated autophagy (Ulgherait et al., 2021), which is another component of the cellular quality control systems (Pohl and Dikic, 2019; Shaid et al., 2013). In this context, the regulation of the hepatic proteasome by 16-h fasting may modulate the function of the cellular quality control systems, which contributes to the health benefits of intermittent fasting. This finding might therefore be helpful to reach a consensus on intermittent fasting programs.

An intriguing finding of the present study is that intermittent fasting initiates the transcriptional circadian resonance of many canonical pathways in the liver. It is assumed that some environmental or behavioral perturbations may trigger transcriptional resonance (Bass, 2012; Bass and Takahashi, 2010). Currently, no typical evidence exists for this concept in animals, but it does occur in *Arabidopsis* (Harmer et al., 2000). Theoretically, intermittent fasting, synchronized daily cycles of fasting and refeeding through the removal and supply of food at a fixed time point, may provoke the transcriptional resonance. However, although it was reported that time-restricted feeding can restore transcriptional rhythmicity in the liver of oscillator-deficient mice (Vollmers et al., 2009), the resonant expression of genes has not hitherto been revealed. One possibility for this is that the resonance in animals may happen on pathways rather than on genes. Here, we did find distinct transcriptional resonances of many canonical pathways in the liver. While the re-establishment of circadian transcription by intermittent fasting has been reported to prevent obesity and metabolic syndrome in mice lacking a circadian clock (Chaix et al., 2019), the importance of the resonance in health still needs to be explored.

Another important finding of the current study is that, analogous to ischemic reperfusion, acute fasting-refeeding may pose a synergistic challenge in mice. Simply from a nutritional perspective, AR is the inverse process of AF. However, it cannot be taken for granted that all the effects of AF can be reversed by AR. The Spearman correlation coefficients of canonical pathways in this study clearly indicated that it was EODR rather than AR that exhibited an obviously negative correlation with AF. From the temporal oscillation curve of resonant

pathways, the effects of AR even looked like a spillover effect of AF. By contrast, we noticed an obvious reverse effect between AR and EODF or AF and EODR. If we consider acute fasting-refeeding as a synergistic challenge, all these phenotypes are logical, and the reverse effects between AR and EODF or AF and EODR reflect the adaptation to acute fasting-refeeding after several daily cycles of fasting and refeeding. The health benefits of intermittent fasting may originate from the adaptation.

In summary, the present work establishes a temporal transcriptional atlas of canonical pathways under five feeding regimens. Fasting for 16 h can awaken a liver-specific cellular quality controller (the proteasome), which coordinates the transcriptional resonance of canonical pathways and may contribute to the health benefits of intermittent fasting. This resource can serve as a basis for targeting the proteasome to reveal the underlying mechanism of intermittent fasting, reaching a consensus on intermittent fasting programs, exploring the transcriptional mechanism of intermittent fasting, and developing intermittent fasting mimics.

Limitations of the study

While this temporal transcriptional atlas of canonical pathways may be helpful to reveal the underlying mechanisms for the health benefits of intermittent fasting, the findings from this study are primarily based on RNA sequencing datasets. Therefore, more experiments, especially genetic and pharmacological loss-of-function experiments targeting the hepatic proteasome, may be needed to further scrutinize the findings. Moreover, additional studies are required to answer several open questions that arise from this study, including what the underlying mechanisms are for the 16-h fasting-dependent and liver-specific proteasome provocation, which factors trigger the pathway resonance, and what the interaction is among proteasome activation, pathway resonance, and health benefits in intermittent fasting.

STAR★METHODS

Detailed methods are provided in the online version of this paper and include the following:

RESOURCE AVAILABILITY

Lead contact—Further information and requests for resources and reagents should be directed to and will be fulfilled by the Lead Contact, Guolin Li (hnsdlgl@hunnu.edu.cn).

Materials availability—This study did not generate new unique reagents.

Data and code availability

- The accession number for the sequences reported in this paper is GEO: GSE154797 (https://www.ncbi.nlm.nih.gov/geo/query/acc.cgi?acc=GSE154797). The DOI for the raw data of blots reported in this paper is 10.17632/x64s7p7cb7.1 (Mendeley Data: https://doi.org/10.17632/x64s7p7cb7.1). These data will be publicly available as of the date of publication.
- This paper does not report original code.

- Any additional information required to reanalyze the data reported in this paper is available from the lead contact upon request.

EXPERIMENTAL MODEL AND SUBJECT DETAILS

Animals—All mouse studies were approved by the Institutional Review Board of the Hunan Normal University and performed according to the Laboratory Animal Resources guidelines. Six-week-old male C57BL/6N mice were purchased from Beijing Vital River Laboratory Animal Technology Co., Ltd. Mice were housed in a temperature-controlled vivarium (25 ± 2°C) on a 12-h light-dark cycle with free access to water and standard rodent chow food (18.9% protein, 5.5% fat, and 61.3% carbohydrate). All experiments were started with 8-week-old mice.

METHOD DETAILS

Intermittent fasting treatment—Mice were randomly grouped to ad libitum (AL) group, acute fasting (AF) group, refeeding after acute fasting (AR) group, every other day fasting (EODF) group, and every other day refeeding (EODR) group. All mice were singly housed for two weeks before study initiation to allow for acclimation to the animal facility. The AL group mice were allowed unrestricted access to food. The mice of AF groups were allowed free access to food except for the last day of acute fasting for 4 h, 8 h, 12 h, 16 h, 20 h, and 24 h, respectively, before being killed. The mice in the AR groups were allowed free access to food except the last two days followed acute fasting for 24 h, and then refeeding for 4 h, 8 h, 12 h, 16 h, 20 h, and 24 h, respectively, before being killed. The mice in the EODF and EODR groups were fed with 15 cycles of alternating 24 h periods of free access to food followed by 24-h fasting, then EODF mice were killed after fasting for 4 h, 8 h, 12 h, 16 h, 20 h, and 24 h, respectively, while EODR mice were killed after refeeding for 4 h, 8 h, 12 h, 16 h, 20 h, and 24 h, respectively. Considering the nocturnal eating characteristics of mice, all fasting and refeeding switches were started at zeitgeber time 12 h.

Western Blot analysis—Frozen liver tissues were lysed in RIPA buffer supplemented with Halt Protease and Phosphatase Inhibitor Cocktail (Servicebio, Wuhan, China) and 1 mM PMSF. Protein concentrations were determined using BCA Protein Assay Kit (Servicebio, Wuhan, China) by a microplate reader (PERL ONG, Beijing, China). Twenty micrograms of protein per lane were loaded onto an 8–12% polyacrylamide Gel and then transferred to PVDF membranes using an electrophoresis chamber (Millipore, Shanghai, China) for 1.5 h. Membranes were blocked in 5% non-fat milk Tris-buffered saline (TBS) followed by overnight incubation in primary antibody at 4°C. Primary antibodies used are as follows: anti-PSMB3 (#K009840P, Solarbio, Beijing, China), anti-PSMB6 (#K003745P, Solarbio, Beijing, China), anti-PSMA4 (#K003378P, Solarbio, Beijing, China) and anti-ATCB (#YT0099, Immunoway, TX, USA). Following primary antibody incubation, blots were washed four times for 10 min each time with TBS and 0.1% Tween 20, and incubated with an anti-rabbit IgG HRP-conjugated secondary antibody (#AS014, ABclonal, Wuhan, China). Blots were stripped with Enhanced Chemiluminescent Liquid (ECL, NCM, Suzhou, China) and re-probed with anti-ATCB for normalization. Blot imaging was performed on a chemiluminescence analyzer (Tanon-5200 Multi, Shanghai, China).

Ketone bodies assays—Serum acetoacetate and β-hydroxybutyrate across the different groups were assessed in a 96-well microplate using commercial ketone bodies assay kits (#BC5060, Solarbio, Beijing, China) and monitored at 340 nm nm with a microplate reader (Perlong, Beijing, China).

RNA extraction and processing—Total RNA was extracted from frozen tissue using TRIzol reagent (Invitrogen) following the manufacturer's instructions. The purity and concentration of the total RNA were determined by a NanoDrop spectrophotometer (ND-1000, Thermo Fisher). The quality/integrity of total RNA was evaluated by a Bioanalyzer (2100, Agilent) with RIN number >7.0, and confirmed by gel electrophoresis.

Library generation and sequencing—Poly(A) RNA was selected from 1 μg total RNA in each sample using Dynabeads Oligo (dT)25 (Thermo Fisher) through two rounds of purification and fragmented into small pieces using Magnesium RNA Fragmentation Module (New England Biolabs) under 94°C for 5–7 min. The cleaved RNA fragments were firstly reverse transcribed using SuperScript™ II Reverse Transcriptase (Invitrogen). Then the second strand of cDNA was synthesized using E. coli DNA polymerase I (New England Biolabs), RNase H (New England Biolabs), and marked with dUTP Solution (Thermo Fisher). Subsequently, after end polishing, A-tailing, adapter ligation, and size selection (using AMPureXP beads), the dUTP-marked strand was selectively degraded by Uracil-DNA-Glycosylase (UDG). The remaining strand was amplified with PCR (95°C for 3 min, 15 cycles of "98°C for 15 s, 60°C for 15 s, and 72°C for 30 s", and 72°C for 5 min) to generate a cDNA library with 300 ± 50 bp. Libraries were multiplexed in equimolar concentrations and sequenced using an Illumina Novaseq™ 6000 with 2 × 150 bp paired-end sequencing (LC-Bio Technology CO., Ltd.) following the vendor's recommended protocol.

Data processing—Quality control was assessed using Cutadapt (Martin, 2011), then HISAT2 aligner (Kim et al., 2015) was used to map reads to the genome (Mus musculus.GRCm38 downloaded from Ensembl). The mapped reads of each sample were assembled using StringTie (Pertea et al., 2015) with default parameters. Finally, fragments per kilobase of exon model per million mapped fragments (FPKM) values were calculated by StringTie and ballgown (Frazee et al., 2015; Pertea et al., 2015). Only genes with the average of FPKM values of the 6 time-points in each feeding regimen >0.1 (Mele et al., 2015) or expressed in at least four samples in each sample group were included in the analysis. One sample from muscle in EODF at ZT20 was excluded from analysis due to RNA degradation.

Rhythmicity assay—Rhythmicity was evaluated with DiscoRhythm (Carlucci et al., 2020) using Cosinor assay (Cornelissen, 2014) and JTK Cycle assay (Hughes et al., 2010). Pathways were considered as rhythmic only when Q values of the JTK Cycle assay were less than 0.01.

Gene set variation analysis (GSVA)—The pathway GSVA scores (Hanzelmann et al., 2013) were calculated from the FPKM values based on 2922 gene sets of canonical pathways that were downloaded from the MSigDB (c2.cp.v7.4) (Mootha et al., 2003;

Subramanian et al., 2005). The differential expression analysis was performed on the whole day GSVA scores using limma (Smyth, 2004). The pathways with $\log_2$(fold change) > $\log_2$(1.5) and adjusted $p < 0.05$ was considered significant.

QUANTIFICATION AND STATISTICAL ANALYSIS

Statistical analysis—All results are expressed as means ± SEM. Computations assumed that all groups were samples from populations with the same scatter. The investigators involved in this study were not completely blinded during sample collection or data analysis in the animal experiments. Outliers were identified by outlier analysis using the ROUT method of Prism 7.0 software and excluded from statistical analyses. Significance was determined by a two-tailed unpaired t test using Prism 7.0 software. A $p < 0.05$ was considered significant.

Supplementary Material

Refer to Web version on PubMed Central for supplementary material.

ACKNOWLEDGMENTS

We thank Qiu Wang, Qian Zhang, Baode Zhu, Guangyao Wu, Lu Wang, Lijiao Zhu, Han Liu, Siyu Wang, Xiaoli Zeng, Yu Liang, Yuebo Wang, Xiaomin Xia, Juan Wang, and Tingting Zhang for assistance with the daily feeding of mice and tissue collection and the LC Science Facility for help with sequencing. G.L. was supported by the National Natural Science Foundation of China (31871198, 31741070) and the Opening Fund of The National & Local Joint Engineering Laboratory of Animal Peptide Drug Development (Hunan Normal University, National Development and Reform Commission). F.W. was supported by the National Natural Science Foundation of China (81903138) and the Natural Science Foundation of Hunan Province (2022JJ30413). The funding sponsors had no role in the writing of the manuscript or in the decision to submit the manuscript for publication.

REFERENCES

Anton SD, Moehl K, Donahoo WT, Marosi K, Lee SA, Mainous AG 3rd, Leeuwenburgh C, and Mattson MP (2018). Flipping the metabolic switch: understanding and applying the health benefits of fasting. Obesity 26, 254–268. 10.1002/oby.22065. [PubMed: 29086496]

Balasse EO, and Fery F (1989). Ketone body production and disposal: effects of fasting, diabetes, and exercise. Diabetes Metab. Rev. 5, 247–270. 10.1002/dmr.5610050304. [PubMed: 2656155]

Bass J (2012). Circadian topology of metabolism. Nature 491, 348–356. 10.1038/nature11704. [PubMed: 23151577]

Bass J, and Takahashi JS (2010). Circadian integration of metabolism and energetics. Science 330, 1349–1354. 10.1126/science.1195027. [PubMed: 21127246]

Carlucci M, Krisciunas A, Li H, Gibas P, Koncevicius K, Petronis A, and Oh G (2020). DiscoRhythm: an easy-to-use web application and R package for discovering rhythmicity. Bioinformatics 36, 1952–1954. 10.1093/bioinformatics/btz834.

Catterson JH, Khericha M, Dyson MC, Vincent AJ, Callard R, Haveron SM, Rajasingam A, Ahmad M, and Partridge L (2018). Short-term, intermittent fasting induces long-lasting gut health and TOR-independent lifespan extension. Curr. Biol. 28, 1714–1724.e4. 10.1016/j.cub.2018.04.015. [PubMed: 29779873]

Chaix A, Lin T, Le HD, Chang MW, and Panda S (2019). Time-restricted feeding prevents obesity and metabolic syndrome in mice lacking a circadian clock. Cell Metab. 29, 303–319.e4. 10.1016/j.cmet.2018.08.004. [PubMed: 30174302]

Challet E (2019). The circadian regulation of food intake. Nat. Rev. Endocrinol. 15, 393–405. 10.1038/s41574-019-0210-x. [PubMed: 31073218]

Cornelissen G (2014). Cosinor-based rhythmometry. Theor. Biol. Med. Model. 11, 16. 10.1186/1742-4682-11-16. [PubMed: 24725531]

Crosby P, Hamnett R, Putker M, Hoyle NP, Reed M, Karam CJ, Maywood ES, Stangherlin A, Chesham JE, Hayter EA, et al. (2019). Insulin/IGF-1 drives PERIOD synthesis to entrain circadian rhythms with feeding time. Cell 177, 896–909.e20. 10.1016/j.cell.2019.02.017. [PubMed: 31030999]

Damiola F, Le Minh N, Preitner N, Kornmann B, Fleury-Olela F, and Schibler U (2000). Restricted feeding uncouples circadian oscillators in peripheral tissues from the central pacemaker in the suprachiasmatic nucleus. Genes Dev. 14, 2950–2961. 10.1101/gad.183500. [PubMed: 11114885]

de Cabo R, and Mattson MP (2019). Effects of intermittent fasting on health, aging, and disease. N. Engl. J. Med. 381, 2541–2551. 10.1056/NEJMra1905136. [PubMed: 31881139]

Di Francesco A, Di Germanio C, Bernier M, and de Cabo R (2018). A time to fast. Science 362, 770–775. 10.1126/science.aau2095. [PubMed: 30442801]

Frazee AC, Pertea G, Jaffe AE, Langmead B, Salzberg SL, and Leek JT (2015). Ballgown bridges the gap between transcriptome assembly and expression analysis. Nat. Biotechnol. 33, 243–246. 10.1038/nbt.3172. [PubMed: 25748911]

Geisler CE, Ghimire S, Bogan RL, and Renquist BJ (2019). Role of ketone signaling in the hepatic response to fasting. Am. J. Physiol. Gastrointest. Liver Physiol. 316, G623–G631. 10.1152/ajpgi.00415.2017. [PubMed: 30767679]

Greenwell BJ, Trott AJ, Beytebiere JR, Pao S, Bosley A, Beach E, Finegan P, Hernandez C, and Menet JS (2019). Rhythmic food intake drives rhythmic gene expression more potently than the hepatic circadian clock in mice. Cell Rep. 27, 649–657.e5. 10.1016/j.celrep.2019.03.064. [PubMed: 30995463]

Hanzelmann S, Castelo R, and Guinney J (2013). GSVA: gene set variation analysis for microarray and RNA-seq data. BMC Bioinformatics 14, 7. 10.1186/1471-2105-14-7. [PubMed: 23323831]

Harmer SL, Hogenesch JB, Straume M, Chang HS, Han B, Zhu T, Wang X, Kreps JA, and Kay SA (2000). Orchestrated transcription of key pathways in Arabidopsis by the circadian clock. Science 290, 2110–2113. 10.1126/science.290.5499.2110. [PubMed: 11118138]

Hatori M, Vollmers C, Zarrinpar A, DiTacchio L, Bushong EA, Gill S, Leblanc M, Chaix A, Joens M, Fitzpatrick JA, et al. (2012). Time-restricted feeding without reducing caloric intake prevents metabolic diseases in mice fed a high-fat diet. Cell Metab. 15, 848–860. 10.1016/j.cmet.2012.04.019. [PubMed: 22608008]

Honjoh S, Yamamoto T, Uno M, and Nishida E (2009). Signalling through RHEB-1 mediates intermittent fasting-induced longevity in C. elegans. Nature 457, 726–730. 10.1038/nature07583. [PubMed: 19079239]

Hughes ME, Hogenesch JB, and Kornacker K (2010). JTK_CYCLE: an efficient nonparametric algorithm for detecting rhythmic components in genome-scale data sets. J. Biol. Rhythms 25, 372–380. 10.1177/0748730410379711. [PubMed: 20876817]

Jassal B, Matthews L, Viteri G, Gong C, Lorente P, Fabregat A, Sidiropoulos K, Cook J, Gillespie M, Haw R, et al. (2020). The reactome pathway knowledgebase. Nucleic Acids Res. 48, D498–D503. 10.1093/nar/gkz1031. [PubMed: 31691815]

Kim D, Langmead B, and Salzberg SL (2015). HISAT: a fast spliced aligner with low memory requirements. Nat. Methods 12, 357–360. 10.1038/nmeth.3317. [PubMed: 25751142]

Kinouchi K, Magnan C, Ceglia N, Liu Y, Cervantes M, Pastore N, Huynh T, Ballabio A, Baldi P, Masri S, and Sassone-Corsi P (2018). Fasting imparts a switch to alternative daily pathways in liver and muscle. Cell Rep. 25, 3299–3314.e6. 10.1016/j.celrep.2018.11.077. [PubMed: 30566858]

Kohsaka A, Laposky AD, Ramsey KM, Estrada C, Joshu C, Kobayashi Y, Turek FW, and Bass J (2007). High-fat diet disrupts behavioral and molecular circadian rhythms in mice. Cell Metab. 6, 414–421. 10.1016/j.cmet.2007.09.006. [PubMed: 17983587]

Li G, Xie C, Lu S, Nichols RG, Tian Y, Li L, Patel D, Ma Y, Brocker CN, Yan T, et al. (2017). Intermittent fasting promotes white adipose browning and decreases obesity by shaping the gut microbiota. Cell Metab. 26, 672–685.e4. 10.1016/j.cmet.2017.08.019. [PubMed: 28918936]

Longo VD, Di Tano M, Mattson MP, and Guidi N (2021). Intermittent and periodic fasting, longevity and disease. Nat. Aging 1, 47–59. 10.1038/s43587-020-00013-3. [PubMed: 35310455]

Manoogian ENC, and Panda S (2017). Circadian rhythms, time-restricted feeding, and healthy aging. Ageing Res. Rev. 39, 59–67. 10.1016/j.arr.2016.12.006. [PubMed: 28017879]

Martin M (2011). Cutadapt removes adapter sequences from high-throughput sequencing reads. EMBnet J. 17, 10–12. 10.14806/EJ.17.1.200.

Mattson MP, Moehl K, Ghena N, Schmaedick M, and Cheng A (2018). Intermittent metabolic switching, neuroplasticity and brain health. Nat. Rev. Neurosci. 19, 63–80. 10.1038/nrn.2017.156.

Meiners S, Heyken D, Weller A, Ludwig A, Stangl K, Kloetzel PM, and Kruger E (2003). Inhibition of proteasome activity induces concerted expression of proteasome genes and de novo formation of Mammalian proteasomes. J. Biol. Chem. 278, 21517–21525. 10.1074/jbc.M301032200. [PubMed: 12676932]

Mele M, Ferreira PG, Reverter F, DeLuca DS, Monlong J, Sammeth M, Young TR, Goldmann JM, Pervouchine DD, Sullivan TJ, et al. (2015). The human transcriptome across tissues and individuals. Science 348, 660–665. 10.1126/science.aaa0355. [PubMed: 25954002]

Mihaylova MM, Cheng CW, Cao AQ, Tripathi S, Mana MD, Bauer-Rowe KE, Abu-Remaileh M, Clavain L, Erdemir A, Lewis CA, et al. (2018). Fasting activates fatty acid oxidation to enhance intestinal stem cell function during homeostasis and aging. Cell Stem Cell 22, 769–778.e4. 10.1016/j.stem.2018.04.001. [PubMed: 29727683]

Mohawk JA, Green CB, and Takahashi JS (2012). Central and peripheral circadian clocks in mammals. Annu. Rev. Neurosci. 35, 445–462. 10.1146/annurev-neuro-060909-153128. [PubMed: 22483041]

Mootha VK, Lindgren CM, Eriksson KF, Subramanian A, Sihag S, Lehar J, Puigserver P, Carlsson E, Ridderstrale M, Laurila E, et al. (2003). PGC-1α-responsive genes involved in oxidative phosphorylation are coordinately downregulated in human diabetes. Nat. Genet. 34, 267–273. 10.1038/ng1180. [PubMed: 12808457]

Mure LS, Le HD, Benegiamo G, Chang MW, Rios L, Jillani N, Ngotho M, Kariuki T, Dkhissi-Benyahya O, Cooper HM, and Panda S (2018). Diurnal transcriptome atlas of a primate across major neural and peripheral tissues. Science 359, eaao0318. 10.1126/science.aao0318. [PubMed: 29439024]

Nencioni A, Caffa I, Cortellino S, and Longo VD (2018). Fasting and cancer: molecular mechanisms and clinical application. Nat. Rev. Cancer 18, 707–719. 10.1038/s41568-018-0061-0. [PubMed: 30327499]

Peek CB, Affinati AH, Ramsey KM, Kuo HY, Yu W, Sena LA, Il-kayeva O, Marcheva B, Kobayashi Y, Omura C, et al. (2013). Circadian clock NAD+ cycle drives mitochondrial oxidative metabolism in mice. Science 342, 1243417. 10.1126/science.1243417. [PubMed: 24051248]

Pertea M, Pertea GM, Antonescu CM, Chang TC, Mendell JT, and Salzberg SL (2015). StringTie enables improved reconstruction of a transcriptome from RNA-seq reads. Nat. Biotechnol. 33, 290–295. 10.1038/nbt.3122. [PubMed: 25690850]

Pohl C, and Dikic I (2019). Cellular quality control by the ubiquitin-proteasome system and autophagy. Science 366, 818–822. 10.1126/science.aax3769. [PubMed: 31727826]

Schneider CA, Rasband WS, and Eliceiri KW (2012). NIH Image to ImageJ: 25 years of image analysis. Nat Methods 9, 671–675. 10.1038/nmeth.2089. [PubMed: 22930834]

Shaid S, Brandts CH, Serve H, and Dikic I (2013). Ubiquitination and selective autophagy. Cell Death Differ. 20, 21–30. 10.1038/cdd.2012.72. [PubMed: 22722335]

Smyth GK (2004). Linear models and empirical bayes methods for assessing differential expression in microarray experiments. Stat. Appl. Genet. Mol. Biol. 3, 1–25. 10.2202/1544-6115.1027.

Soares ROS, Losada DM, Jordani MC, Evora P, and Castro-e-Silva O (2019). Ischemia/reperfusion injury revisited: an overview of the latest pharmacological strategies. Int. J. Mol. Sci. 20, 5034. 10.3390/ijms20205034.

Stekovic S, Hofer SJ, Tripolt N, Aon MA, Royer P, Pein L, Stadler JT, Pendl T, Prietl B, Url J, et al. (2019). Alternate day fasting improves physiological and molecular markers of aging in healthy, non-obese humans. Cell Metab. 30, 462–476.e6. 10.1016/j.cmet.2019.07.016. [PubMed: 31471173]

Stokkan KA, Yamazaki S, Tei H, Sakaki Y, and Menaker M (2001). Entrainment of the circadian clock in the liver by feeding. Science 291, 490–493. 10.1126/science.291.5503.490. [PubMed: 11161204]

Subramanian A, Tamayo P, Mootha VK, Mukherjee S, Ebert BL, Gillette MA, Paulovich A, Pomeroy SL, Golub TR, Lander ES, and Mesirov JP (2005). Gene set enrichment analysis: a knowledge-based approach for interpreting genome-wide expression profiles. Proc. Natl. Acad. Sci. USA 102, 15545–15550. 10.1073/pnas.0506580102. [PubMed: 16199517]

Tanaka K (2009). The proteasome: overview of structure and functions. Proc. Jpn. Acad. Ser. B Phys. Biol. Sci. 85, 12–36. 10.2183/pjab.85.12.

Ulgherait M, Midoun AM, Park SJ, Gatto JA, Tener SJ, Siewert J, Klickstein N, Canman JC, Ja WW, and Shirasu-Hiza M (2021). Circadian autophagy drives iTRF-mediated longevity. Nature 598, 353–358. 10.1038/s41586-021-03934-0. [PubMed: 34588695]

Venables WN, and Ripley BD (2002). Modern Applied Statistics with S, Fourth edition (Springer). 10.1007/978-0-387-21706-2.

VerPlank JJS, Lokireddy S, Zhao J, and Goldberg AL (2019). 26S Proteasomes are rapidly activated by diverse hormones and physiological states that raise cAMP and cause Rpn6 phosphorylation. Proc. Natl. Acad. Sci. USA 116, 4228–4237. 10.1073/pnas.1809254116. [PubMed: 30782827]

Villanueva JE, Livelo C, Trujillo AS, Chandran S, Woodworth B, Andrade L, Le HD, Manor U, Panda S, and Melkani GC (2019). Time-restricted feeding restores muscle function in Drosophila models of obesity and circadian-rhythm disruption. Nat. Commun. 10, 2700. 10.1038/s41467-019-10563-9. [PubMed: 31221967]

Vollmers C, Gill S, DiTacchio L, Pulivarthy SR, Le HD, and Panda S (2009). Time of feeding and the intrinsic circadian clock drive rhythms in hepatic gene expression. Proc. Natl. Acad. Sci. USA 106, 21453–21458. 10.1073/pnas.0909591106. [PubMed: 19940241]

Xie K, Neff F, Markert A, Rozman J, Aguilar-Pimentel JA, Amarie OV, Becker L, Brommage R, Garrett L, Henzel KS, et al. (2017). Every-other-day feeding extends lifespan but fails to delay many symptoms of aging in mice. Nat. Commun. 8, 155. 10.1038/s41467-017-00178-3. [PubMed: 28761067]

Yang X, Downes M, Yu RT, Bookout AL, He W, Straume M, Mangelsdorf DJ, and Evans RM (2006). Nuclear receptor expression links the circadian clock to metabolism. Cell 126, 801–810. 10.1016/j.cell.2006.06.050. [PubMed: 16923398]

Zhang R, Lahens NF, Ballance HI, Hughes ME, and Hogenesch JB (2014). A circadian gene expression atlas in mammals: implications for biology and medicine. Proc. Natl. Acad. Sci. USA 111, 16219–16224. 10.1073/pnas.1408886111. [PubMed: 25349387]

Highlights

- Canonical pathways are highly rhythmic and sensitive to feeding regimens
- Fasting for 16 h awakens a liver-specific quality controller
- Fasting for 16 h triggers circadian resonance of canonical pathways
- The hepatic proteasome is a fasting “timer” and coordinator of pathway resonance

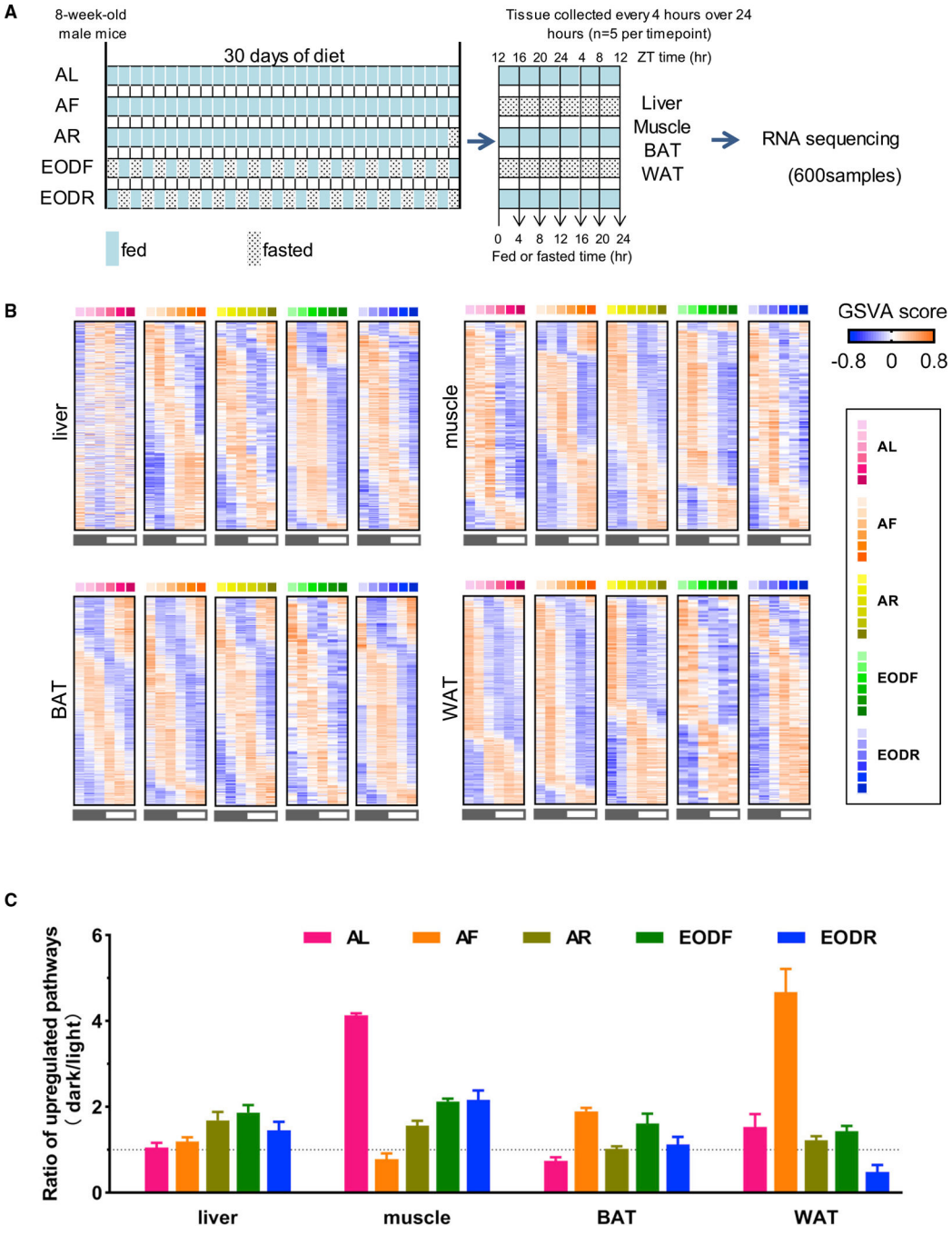

Figure 1. Canonical pathway profiling of mouse tissues reveals tissue-specific oscillating signatures in intermittent fasting

(A) Experimental design. Four metabolic tissues (liver, skeletal muscle [biceps femoris], interscapular brown adipose tissue [BAT], and inguinal white adipose tissue [WAT]) were collected every 4 h across the light/dark cycle from a single cohort of C57BL/6N mice. Six time points were profiled for all these tissues. n = 5 mice/group.

(B) Heatmaps showing tissue-specific and feeding-regimen-specific oscillatory pathways in four metabolic tissues. Cells were shaded according to GSVA scores (blue, downregulated; red, upregulated). Six columns in each heatmap from left to right are zeitgeber time (ZT) 16,

ZT20, ZT0, ZT4, ZT8, and ZT12, respectively. The dark/light cycle was indicated by black and white bars (black, dark; white, light). Feeding regimens were indicated on the top of each heatmap (each color from light to dark represented feeding or fasting duration from 4 to 24 h with a step of 4 h). n = 5 mice/group.

(C) Tissue-specific dark/light ratio of upregulated pathways under different feeding regimens. Data are presented as mean ± SEM (n = 5 mice/group). AF, acute fasting; AL, *ad libitum*; AR, refeeding after acute fasting; BAT, brown adipose tissue; EODF, every-other-day fasting; EODR, every-other-day refeeding; GSVA, gene set variation analysis; WAT, white adipose tissue (see also Figures S1 and S2 and Tables S1 and S2).

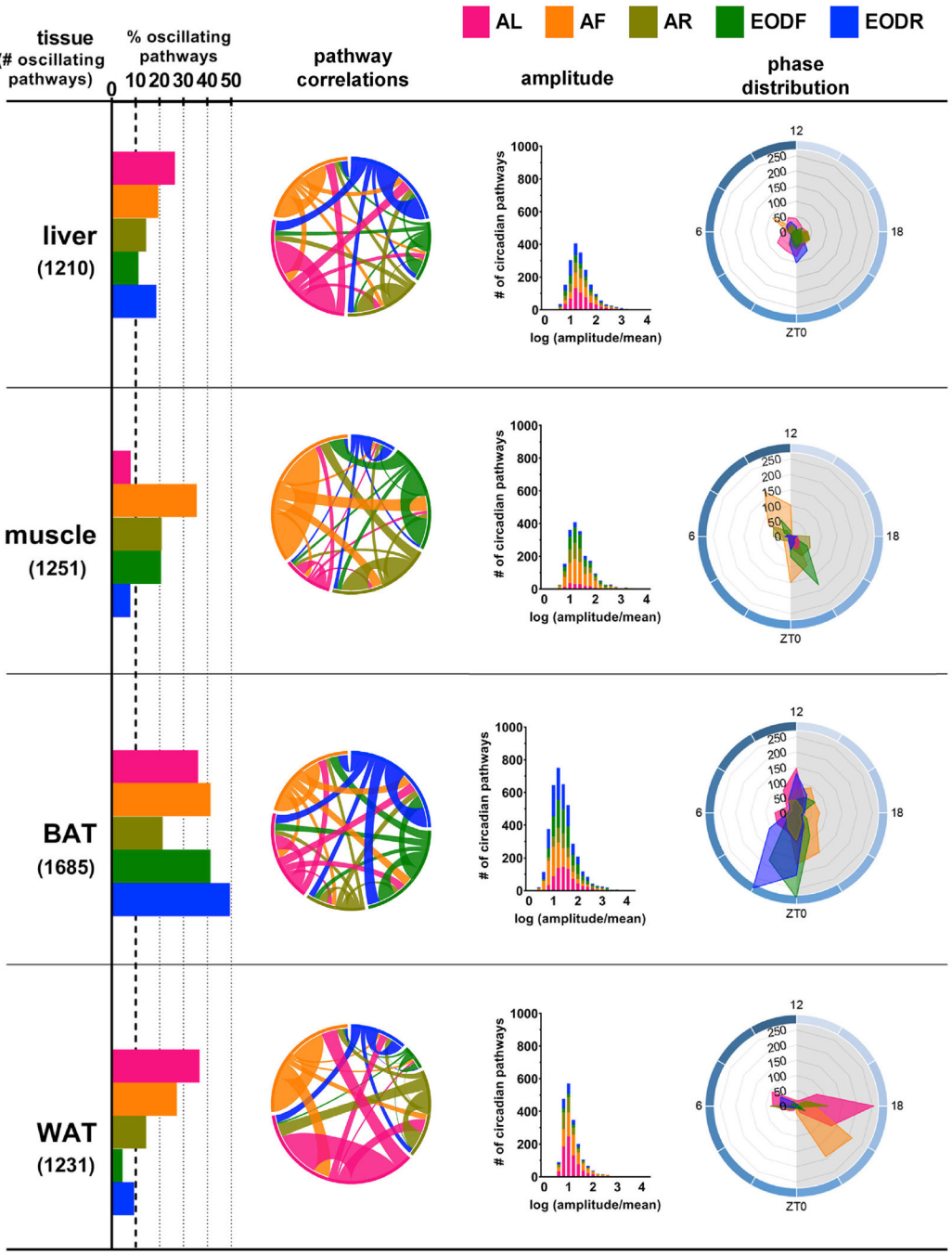

Figure 2. Comparative analysis of circadian oscillating pathways highlights the tissue-specific response to different feeding regimens

Circadian oscillating pathways ($Q < 0.01$, Jonckheere-Terpstra-Kendall [JTK] cycle) for each tissue were plotted from left to right according to (1) total number of (#) oscillating pathways, (2) relative percentage of (%) oscillating pathways to detected pathways, (3) graphical summary of the correlations of oscillating pathways across different feeding regimens (ribbon thickness represents the number of correlated pathways), (4) amplitude of oscillation, and (5) phase distribution (the numbers outside the circle are ZTs; the blue-colored circle from light to dark refer to the fasting or feeding time from 0 to 24 h with

the step of 2 h; gray indicates the dark cycle; the numbers inside radial plot are the number of cycling pathways; different colors of radial plots refer to different feeding regimens as indicated on the top). n = 5 mice/group (see also Tables S2 and S3).

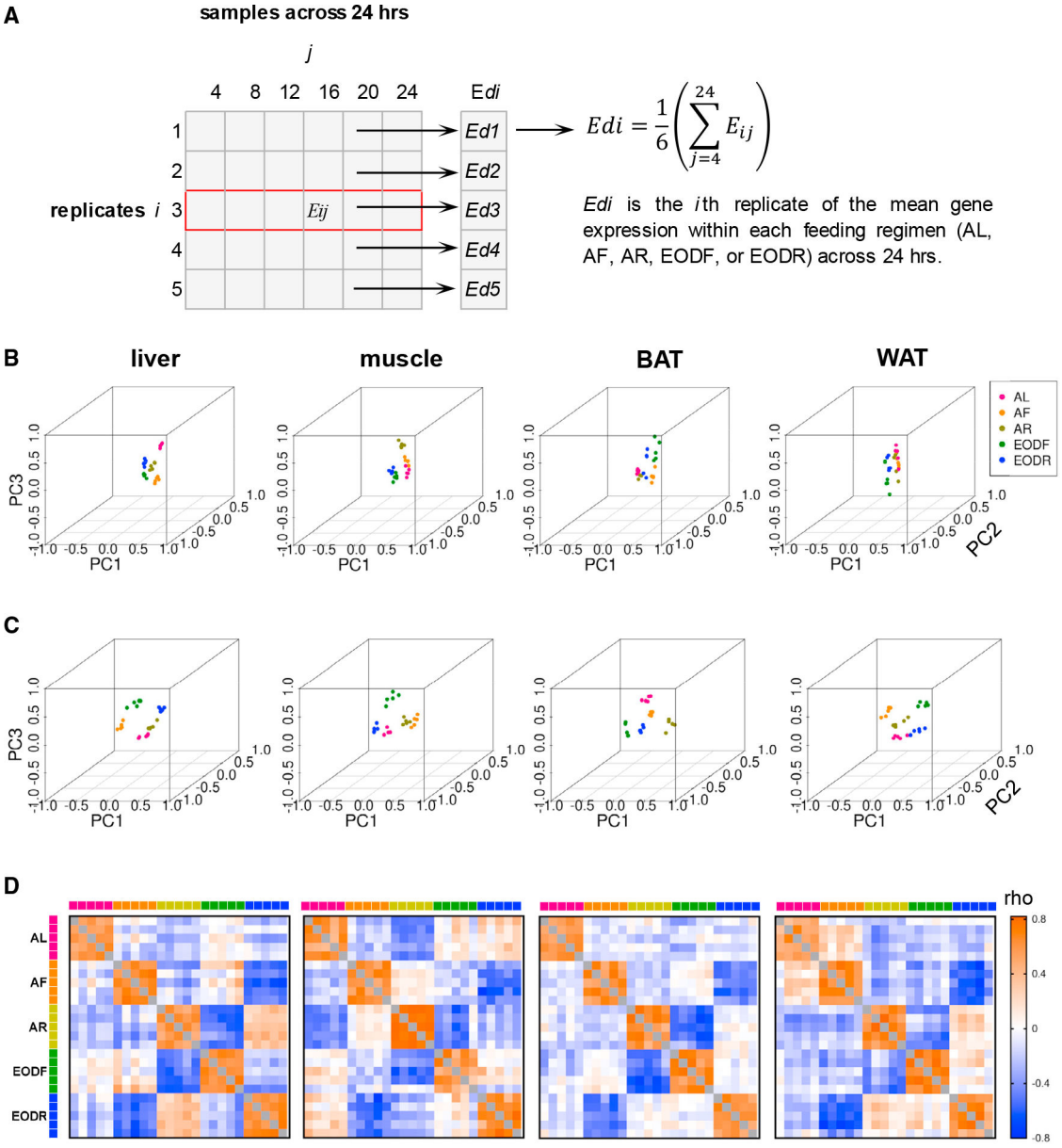

Figure 3. Canonical pathway profiling all day suggests an adaptation to acute fasting-refeeding in intermittent fasting

(A) Data processing. The mean expression values of genes throughout the whole day were calculated from the expression values of six time points in a 24-h day within each feeding regimen and tissue. n = 5 mice/group.

(B and C) The 3D-PCA plots of classes of the whole day gene expression (B) and pathway GSVA score (C) derived from five feeding regimens. n = 5 mice/group.

(D) The pathway Spearman correlation heatmaps showing the evident negative correlation of AF with EODR or AR with EODF in all four metabolic tissues. Cells were shaded according to pathway Spearman correlation coefficients (blue, negative; red, positive) that were calculated from the whole-day GSVA scores. Feeding regimens are indicated on the

left and/or the top of each heatmap (each color represents a feeding regimen, and each cell refers to a replicate). n = 5 mice/group.

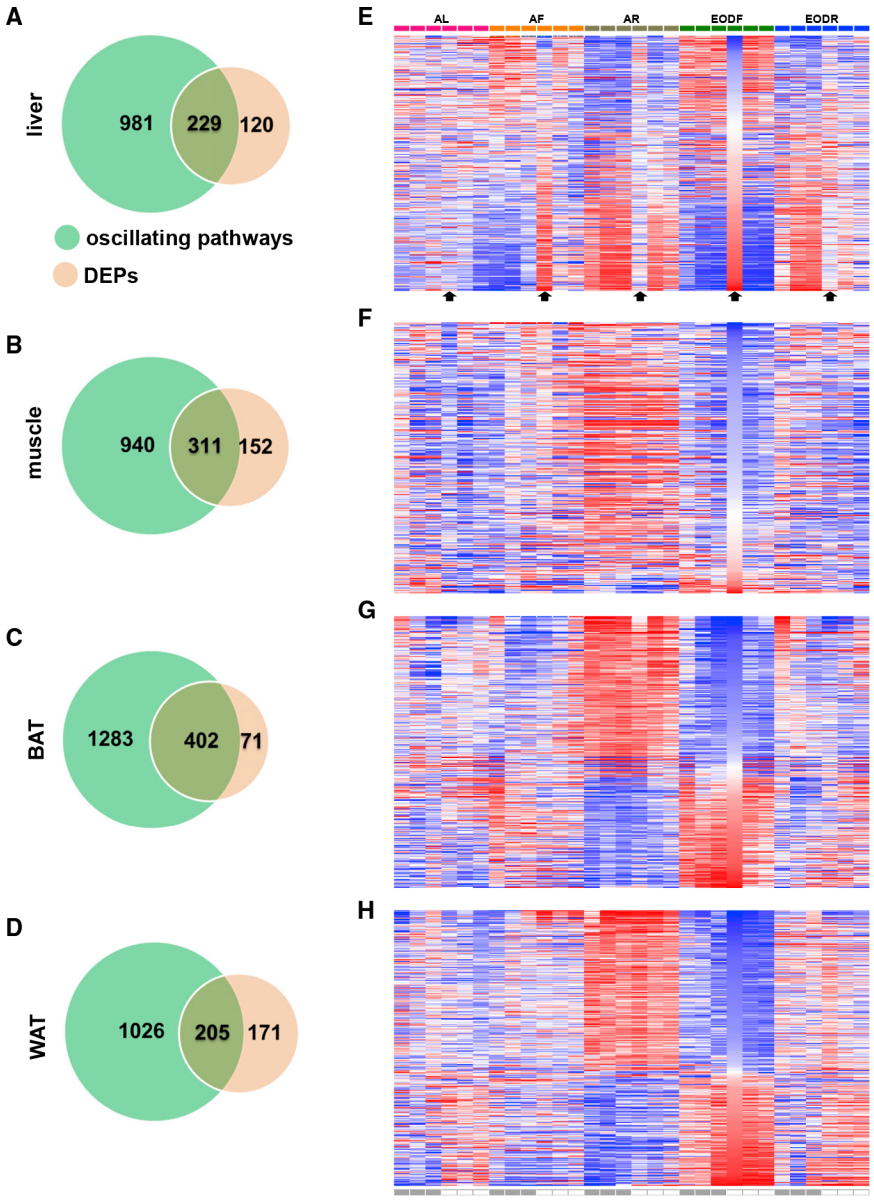

Figure 4. FRPs exhibit a manifest switch after 16 h fasting or refeeding in the liver

(A–D) The overlap of oscillating pathways (green) and DEPs (brown) in the liver (A), muscle (B), BAT (C), and WAT (D). Numbers in the overlapping regions are the number of FRPs (that is, pathways with both oscillating and differentially expressed), and other numbers in the circle are the number of pathways showing only oscillating or differentially expressed, respectively. n = 5 mice/group.

(E–H) Heatmap exhibiting the changes of GSVA scores of FRPs across different times of five feeding regimens in the liver (E), muscle (F), BAT (G), and WAT (H). Black arrows referred to the 16th hour of treatments (fasting or feeding), which was equal to the ZT4. Top color bars, different feeding regimens; bottom filled bars, dark; hollow bars, light. n = 5 mice/group. DEPs, differentially expressed pathways; FRPs, functional rhythmic pathways (see also Tables S2 and S4).

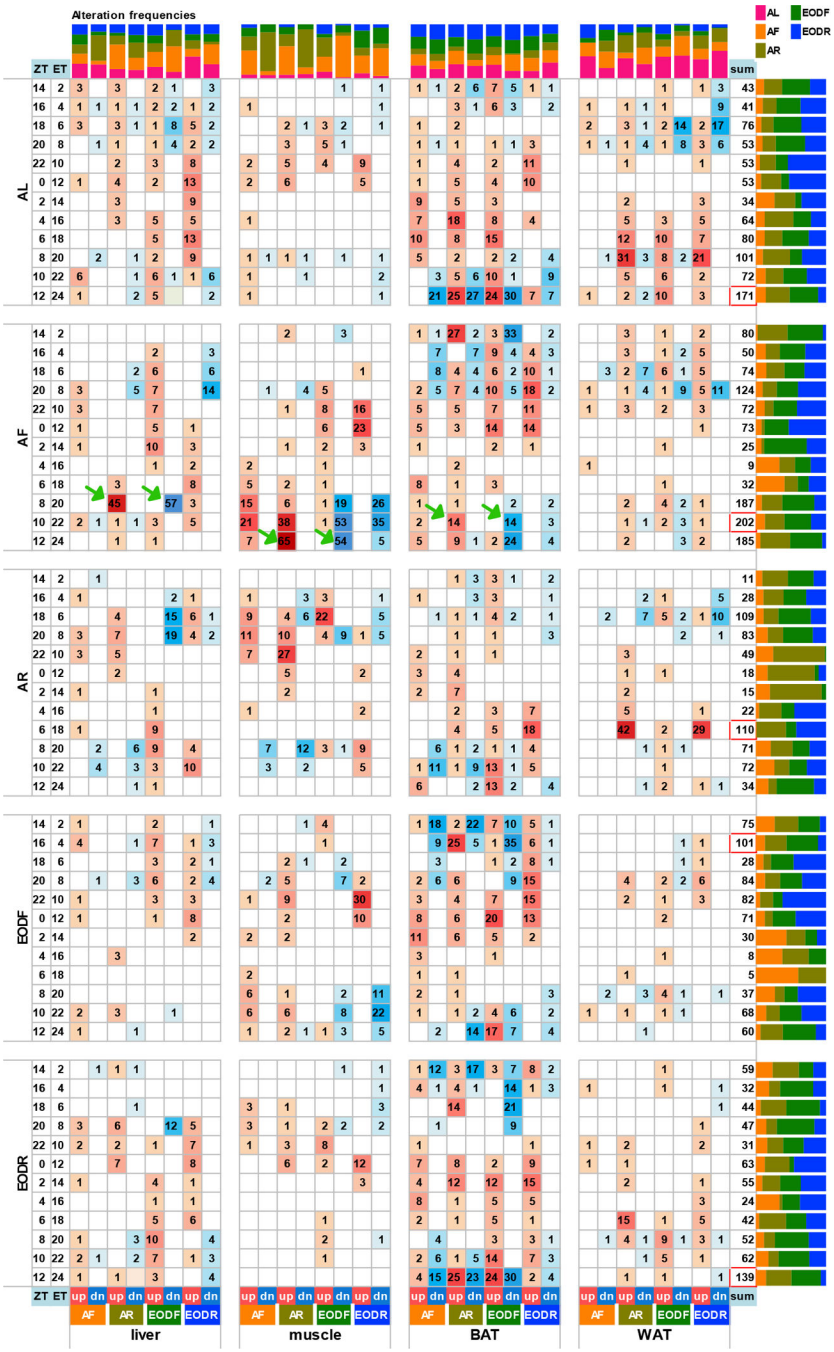

Figure 5. Intersection of oscillating and DEPs

Detailed heatmap of alteration frequencies in numbers displaying the intersections of the oscillating pathways (rows) and DEPs (columns) in different feeding regimens and tissues. Each column shows the distribution of DEPs by feeding-regimen-specific oscillating phases, and each row shows the distribution of phase-specific oscillating pathways by feeding-regimen-specific DEPs. Red, upregulated events; blue, downregulated events (color intensity increases with the frequency of occurrence). Color top bar charts show the fraction of feeding-regimen-specific oscillating pathways in DEPs of a specific feeding regimen

and tissue. Color side bar charts show the fraction of feeding-regimen-specific DEPs in each phase of oscillating pathways in a specific feeding regimen. n = 5 mice/group. dn, downregulated; ET, executing time duration for fasting or feeding; up, upregulated (see also Figure S3 and Tables S2 and S3).

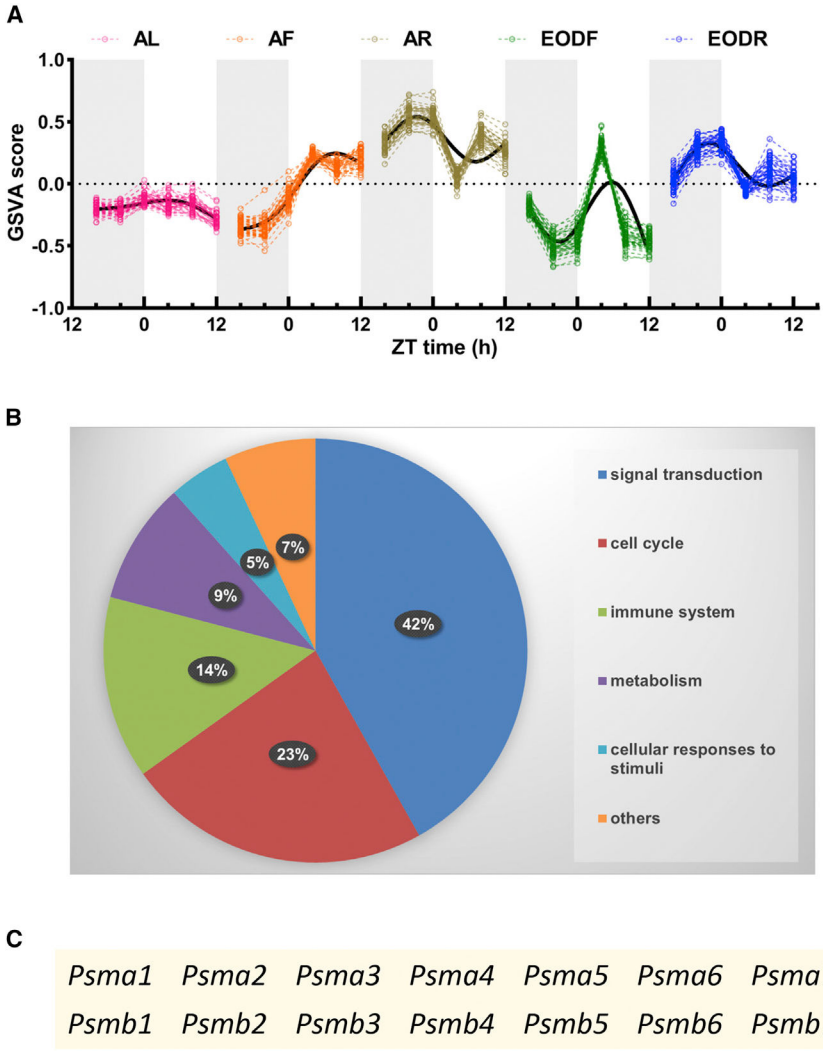

Figure 6. Circadian resonance of 43 pathways in the liver highlights a proteasome switch in intermittent fasting

(A) The circadian resonance of 43 functional pathways in the liver of AF mouse. n = 5 mice/group.

(B) The categories of the 43 resonant functional pathways according to the Reactome Pathway Database.

(C) List of shared genes by the 43 resonant functional pathways (see also Figure S2 and Table S2).

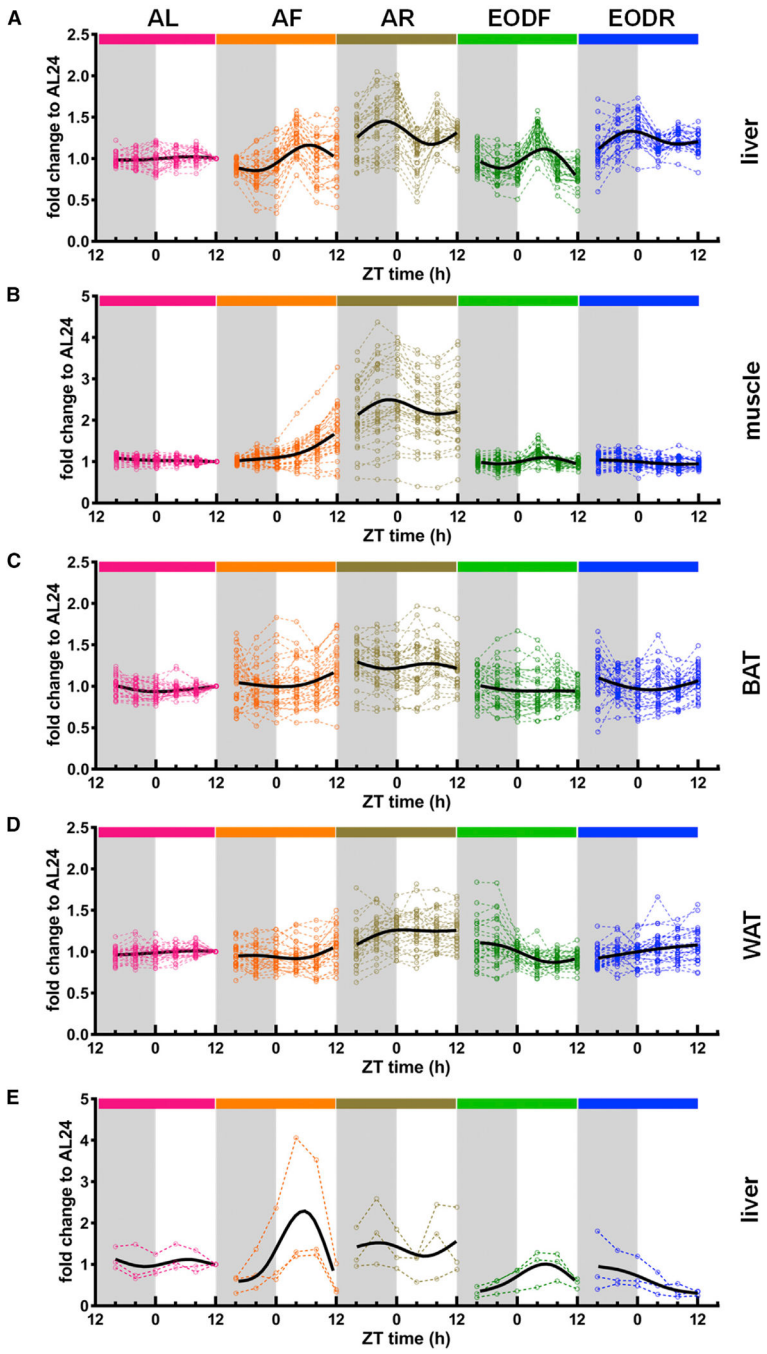

Figure 7. Circadian transcriptional changes of proteasome subunits confirm the switching effect after 16 h of fasting or refeeding in the liver

(A–D) The circadian transcriptional changes of proteasome subunits under different feeding regimens in the liver (A), muscle (B), BAT (C), and WAT (D). Each dotted red line refers to a proteasome subunit, and the black line refers to the average trend of all proteasome subunits. Shadow, dark; blank, light. n = 5 mice/group.

(E) The circadian transcriptional changes of three proteasome proteins under different feeding regimens in the liver. Each dotted red line refers to normalized mean densitometry values of a proteasome protein from western blot in Figure S4, and the black line refers to

the average trend of all three proteasome proteins. Densitometry values were normalized to actin beta (ACTB) expression for each lane and presented as fold change of AL24 mice. Shadow, dark; blank, light. n = 2 mice/group (see also Figures S4, S5, and S6 and Tables S1 and S5).

KEY RESOURCES TABLE

REAGENT or RESOURCE	SOURCE	IDENTIFIER
Antibodies		
Rabbit PSMB3 antibody	Beijing Solarbio Science & Technology Co., Ltd	Cat# K009840P
Rabbit PSMB6 antibody	Beijing Solarbio Science & Technology Co., Ltd	Cat# K003745P
Rabbit PSMA4 antibody	Beijing Solarbio Science & Technology Co., Ltd	Cat# K003378P
Rabbit Actin β Polyclonal antibody	ImmunoWay Biotechnology Co.	Cat# YT0099; RRID:AB_2885029
HRP Goat Anti-Rabbit IgG (H + L)	CliniSciences	Cat# AS014; RRID:AB_2769854
Chemicals, peptides, and recombinant proteins		
Anhydrous ethanol	Sinopharm Chemical Reagent Beijing Co Ltd	Cat# c003860
Alcohol isopropyl	Sinopharm Chemical Reagent Beijing Co Ltd	Cat#CFSR-40049962
β-Mercaptoethanol	Sinopharm Chemical Reagent Beijing Co Ltd	Cat# 0482
Critical commercial assays		
AMPureXP beads	Beckman	Cat# A63881
Dynabeads Oligo (dT)25-61005	Thermo Fisher	Cat# 61005
dUTP Solution	Thermo Fisher	Cat# R0133
E. coli DNA polymerase I	New England Biolabs	Cat# M0209
Magnesium RNA Fragmentation Module	New England Biolabs	Cat# E6150
RNase H	New England Biolabs	Cat# M0297
Uracil-DNA Glycosylase	New England Biolabs	Cat# M0280
SuperScript™ II Reverse Transcriptase	Invitrogen	Cat# 1896649
Ketone body Assay Kit	Beijing Solarbio Science & Technology Co., Ltd	Cat# BC5060
Enhanced Chemiluminescent Kit	New Cell & Molecular Biotech Co., Ltd	Cat# P10300
Deposited data		
RNA sequencing data	This paper	GEO: GSE154797
Western Blot data	This paper; Mendeley Data	Mendeley Data: https://doi.org/10.17632/x64s7p7cb7.1
Experimental models: Organisms/strains		
Mouse: C57BL/6N	Beijing Vital River Laboratory Animal Technology Co., Ltd.	Strain Code: 213
Software and algorithms		
ImageJ	Schneider et al., 2012	https://imagej.nih.gov/ij/; RRID:SCR_003070
cutadapt-1.9	https://cutadapt.readthedocs.io/en/stable/	https://doi.org/10.14806/ej.17.1.200; RRID: SCR_011841
DESeq2	http://www.bioconductor.org/packages/release/bioc/html/DESeq2.html	https://doi.org/10.18129/B9.bioc.DESeq2; RRID:SCR_015687
DiscoRhythm 1.2.1	https://mcarlucci.shinyapps.io/discorhythm/	N/A

REAGENT or RESOURCE	SOURCE	IDENTIFIER
edgeR	https://bioconductor.org/packages/release/bioc/html/edgeR.html	https://doi.org/10.18129/B9.bioc.edgeR
GraphPad Prism 7.0	http://www.graphpad.com/	RRID:SCR_002798
gffcompare-0.9.8.Linux_x86_64	http://ccb.jhu.edu/software/stringtie/gffcompare.shtm	N/A
HISAT2-2.0.4	https://daehwankimlab.github.io/hisat2/	RRID:SCR_015530
StringTie-1.3.4d.Linux_x86_64	http://ccb.jhu.edu/software/stringtie/	RRID:SCR_016323
GSVA 1.42.0	https://www.bioconductor.org/packages/release/bioc/html/GSVA.html	https://doi.org/10.18129/B9.bioc.GSVA; RRID:SCR_021058
scatterplot3d 0.3.41	https://cran.r-project.org/web/packages/scatterplot3d/index.html	https://doi.org/10.18637/jss.v008.i11
STAT 0.1.0	https://cran.r-project.org/web/packages/STAT/index.html	N/A
limma 3.50.0	https://bioconductor.org/packages/release/bioc/html/limma.html	https://doi.org/10.18129/B9.bioc.limma; RRID:SCR_010943
Circos online	http://mkweb.bcgsc.ca/tableviewer/	RRID:SCR_011798